Prescribed fire selects for a pyrophilous soil subcommunity in a northern California mixed conifer forest.

Monika S. Fischer[1], Neem J. Patel[1], Phillip J. de Lorimier, and Matthew F. Traxler*

Department of Plant and Microbial Biology, University of California, Berkeley, Berkeley 94720, USA.

[1]These authors contributed equally.

*Correspondence:

mtrax@berkeley.edu

University of California, Berkeley

111 Koshland Hall

Berkeley CA 94720

ABSTRACT

Low intensity prescribed fire is a critical strategy for mitigating the effects of catastrophic wildfires. The above-ground response to fire has been well-documented, including many ecosystem benefits associated with prescribed burning, but fewer studies have directly addressed the effect of prescribed fire on soil organisms. We aimed to understand how soil microbial communities respond to prescribed fire and to determine the ecological processes driving their dynamics. We extensively sampled four plots for 17 months in a mixed conifer forest in northern California, USA; immediately following a low-intensity prescribed fire, a higher-intensity prescribed fire, and two no-burn control plots. We found that prescribed fire significantly altered the community structure for both fungi (ITS) and bacteria (16S), which was sustained throughout the time-series. By comparing our community profiling results with a model of neutral community assembly, we found that the presence of most taxa across all experimental conditions could be explained by neutral processes. However, combining threshold indicator taxa analysis and correlation network analysis with the neutral model identified a cohort of taxa that responded deterministically to prescribed fire. The subcommunity identified through this series of analyses includes both known and new pyrophilous taxa. Beyond this, our analyses revealed network modules within postfire communities which were responsive to fire-intensity. Taken together, these results lay the foundation for building a process-driven understanding of microbial community assembly in the context of the classical disturbance regime of fire.

INTRODUCTION

Under the current trajectory of climate change, wildfires are expected to continue increasing in frequency and severity in western North America and other regions across the globe [1–3]. Wildfires burn hundreds of millions of hectares of vegetation annually [4] and contribute to the global carbon cycle both in terms of atmospheric input as CO_2 and terrestrial sequestration of carbon in the form of pyrogenic organic matter (PyOM) [5–7]. A key strategy toward decreasing the frequency of devastating wildfires is the implementation of lower-intensity prescribed fires and managed wildfires. These lower-intensity controlled

43 burns have proven effective in reducing the fuel load and the likelihood of catastrophic fire [8–10]. While
44 the effects of prescribed fire on plant and animal communities are increasingly well-documented [9–13],
45 our understanding of the impact of fire management strategies on microbial communities is much more
46 limited [14]. In this study, we investigated the effects of prescribed burns on soil bacteria and fungi with
47 the aim of understanding the ecological processes that shape these communities.

48 Several key ecological processes operate together to dictate community assembly after
49 perturbations such as fire. One process by which communities assemble is the deterministic (or 'niche')
50 process of ecological selection, which encompasses environmental filtering and biotic competition. In
51 contrast, neutral (or random) processes of community assembly include dispersal, drift, and speciation [15].
52 Understanding the relative contributions of these processes to community assembly after disturbance is
53 critical because; (1) they ultimately determine the successional trajectory and recovery time of these
54 communities, and (2) possible interventions designed to enhance community resilience will likely need to
55 take these processes into account if they are to be successful. When a new habitat becomes available for
56 microbial colonization, neutral processes typically dominate early on, with selection playing a more
57 important role over time [16, 17]. Fire can be among the most extreme types of disturbance, effectively
58 resulting in a new habitat that is recolonized over time via secondary succession [18]. Consistent with this
59 notion, Ferrenberg, *et al* found that neutral processes played a strong role in soil bacterial communities four
60 weeks after severe wildfire, and after sixteen weeks the community was less neutral [17].

61 Work across multiple post-fire systems (predominantly wildfire) is starting to paint a complex
62 picture of the impacts of fire on microbial communities. Despite complete decimation of the above-ground
63 ecosystem, many organisms are able to survive below ground, even during the most extreme wildfires [12].
64 A recently proposed conceptual model provides a framework for considering the thermo-chemical gradient
65 that defines the post-fire soil habitat [19]. This model describes the insulative capacity of soil, meaning that
66 the effect of fire decreases with depth, and organisms below a certain depth are protected from the heat of
67 the fire by the soil itself. Despite survival at deeper depths, the organisms present near the soil surface are
68 generally dramatically impacted by fire. The documented effects of fire on the soil microbial community

include a decrease in overall biomass [20–22] and a significant perturbation of the community structure [23–27]. Both fungal and bacterial communities have been observed to decrease in richness after severe wildfire [23–25, 27], although there are notable exceptions [26].

Over a hundred years of macroscopic observation [28–30], combined with recent community DNA sequencing studies, suggest that a distinct pyrophilous fungal community assembles in wildfire-affected soils. These pyrophilous fungi produce abundant fruiting bodies commonly seen on the surfaces of burnt soil and pyrolyzed wood, and more recently these taxa have also been identified via DNA sequencing of post-fire soils [19, 24–27, 31–38]. Commonly observed pyrophilous fungi include members of the genera *Pyronema*, *Anthracobia, Geopyxis*, *Tricharina, Morchella*, *Peziza, Pholiota*, *Lyophyllum, Myxomphalia,* and *Neurospora.* Comparatively less is known about bacterial taxa that respond positively in post-fire soils, although taxa that appear across recent studies include *Paraburkholderia*, *Arthrobacter*, *Flavobacterium*, and *Massilia* [25–27]. To our knowledge, only one recent study has investigated the effect of prescribed fire on both soil fungal and bacterial communities. Mino *et al* conducted ten replicate low- and high-intensity prescribed fires in a shrub-encroached prairie ecosystem, and analyzed samples from two time points; pre-fire and post-fire [31]. They found that high-intensity fire, but not low-intensity fire, reduced richness of both bacteria and fungi. Additionally, the bacteria *Massilia*, *Domibacillus*, and the fungi *Neurospora*, *Pyronema*, *Anthracobia*, and *Penicillium* were significant indicators of post-fire samples [31]. Beyond this example, soil microbial community assembly after prescribed burns has not been deeply explored.

In this work, we sought to address two major questions. First, does prescribed fire lead to assembly of a community of pyrophilous organisms similar to those seen after severe wildfires? And second, what ecological processes drive formation of the community after prescribed fire? To answer these questions, we deeply sampled two prescribed burn plots and two no-burn control plots over 17 months in a mixed conifer forest in the Sierra Nevada mountains of northern California, USA. Combining threshold indicator taxa analysis (TITAN), correlation network analysis, and a model of neutral community assembly delineated a group of taxa whose presence is likely explained by a deterministic response to prescribed fire.

Importantly, many members of this pyrophilous subcommunity have been previously described as responding positively after wildfire, and our analyses add several new taxa to the ranks of potentially pyrophilous microbes. While this pyrophilous subcommunity likely assembled as the result of selective processes following prescribed fire, we find that the majority of the postfire community is likely assembled as the result of neutral processes. This work provides a foundation for building a mechanistic understanding of the ecological processes that shape post-fire microbial communities.

MATERIALS & METHODS

Prescribed fire treatments

Prescribed fires were conducted at the University of California's Blodgett Forest Research Station located near Georgetown, CA, USA. Blodgett Forest is a mixed conifer forest (mostly *Pinus lambertiana*, *Pinus ponderosa*, and *Pseudotsuga menziesi*, with some scattered *Calocedrus decurrens, Sequoiadendron giganteum*, *Abies concolor*, and *Quercus kelloggii*). Soil is in the Holland series, generally characterized as fine-loamy, mixed, mesic Ultic Haploxeralfs. We established four 10m transects within the forest at roughly 1360m elevation; Hi (38.89598, -120.64800), Lo (38.90016, -120.65648), 1c (38.90562, -120.66345), and 2c (38.90191, -120.65901). The Hi plot was treated with a high-intensity slash-pile burn on 4 Jan 2019. The Lo plot was treated with a low-intensity broadcast burn on 25 Oct 2018, and plot 2c was treated with a moderate-intensity broadcast burn on 13 Feb 2020. All prescribed burns were facilitated with fossil fuel drip torches. Fossil fuel was excluded from transects, instead, ignited fossil fuel was dripped at least two meters away, and fire naturally traveled across our transects as it burned through dry plant debris. To measure soil temperature during and after fire, we buried Extech SDL200 data loggers ~0.5m below the soil surface, and ~2-3m away from our sampling transect. Each data logger was equipped with four thermocouples, and the data loggers were protected inside a hard plastic shoebox with a hole cut in the side to allow the thermocouples to exit. Temperature was measured every minute until the batteries died (roughly four days).

Sample collection

Transect sampling locations were randomly assigned without replacement for each plot for the entirety of our sampling time-series. Prior to burning, and in control plots, 10cm soil cores were collected using an ethanol-sterilized soil sampler (JMC PN031). After burning, we collected soil core samples from 0-3cm and 3-6cm. Sampling depths were initially determined based on previous work [19] and the data from our thermocouples. We also conducted a pilot experiment in plot 2c to directly test if sampling depth affected the resulting observed microbial community. For this pilot experiment, six replicate soil samples were collected from the following depths at two time points pre- and post-fire; 0-1cm, 1-2cm, 2-3cm, 3-4cm, 4-5cm, 5-10cm, and 10-20cm. In addition, we later pooled equivalent amounts of soil from 0-3cm and from 0-10cm prior to DNA extraction. Figure S1 and S2 illustrate that there were no significant differences in the composition or diversity of the microbial communities observed at the scale of 0-20cm in Blodgett soil. (PERMANOVA $p > 0.05$, and ANOVA $p > 0.1$, $n = 6$).

All plots were sampled at every time point. Triplicate soil samples were collected at least once immediately prior to burning, once immediately after burning, and then once/month thereafter. To capture community dynamics associated with the first precipitation event, we increased our sampling frequency during the weeks following the first precipitation event and the start of the wet season in late November 2018. Multiple cores were collected per sample and immediately pooled in a 50mL conical tube, to a total volume of ~25-30mL of soil. After collection, samples were transported by car and immediately placed in a -80 ºC freezer. pH was measured using a soil to water ratio of 1:2.5 within 48 hours of sample collection.

DNA extraction, PCR amplification, and sequencing

We generally followed the methodology described by Simmons, *et al* [39]. To isolate total gDNA from soil, 1.2-1.5g of soil was transferred to a 2mL eppendorf tube and then we followed the Qiagen PowerSoil DNA extraction kit protocol. We eluted the gDNA on 100ul of DEPC water. 5ng/ul of DNA was used for simultaneous PCR amplification and illumina library prep with dual 12bp barcodes. Primer sequences in File S1 [39–41]. Samples were randomly assigned barcodes, and randomly distributed

147 spatially across PCR plates (excluding corners) and sequencing libraries. 100ng of DNA from each sample
148 was pooled to form a library. Libraries were sequenced via a PE300 strategy on illumina MiSeq, and then
149 the resulting data were demultiplexed at the UC Davis Genome Center.
150
151 *Raw sequence processing*
152 For the ITS sequences, we used AMPtk v1.5.1 (which used VSEARCH v2.15.0) to quality filter
153 reads, trim off primer sequences, and merge forward and reverse reads together [42]. Merged reads less
154 than 100bp were filtered out, and remaining reads were trimmed to 300bp. We then used DADA2 v1.14
155 (via R v4.0.3) to dereplicate the sequences, infer Amplicon Sequence Variants (ASVs), remove chimeras,
156 assign taxonomy, and ultimately build the tables used in downstream analyses: OTU table, taxonomy table,
157 and sequence table [43, 44]. The UNITE v.8.3 database was used to assign fungal taxonomy, and FUNGuild
158 added functional guild information for many taxa [45, 46]. For 16S sequences, we used Quantitative
159 Insights into Microbial Ecology version 2 (QIIME2 v2021.8) for all our read processing steps [47]. We
160 used built-in tools to quality filtered reads and to trim reads where the quality score was < 25. QIIME2
161 incorporates cutadapt [48] to remove primer sequences and merge reads using the default parameters. The
162 DADA2 [43] step in the QIIME2 pipeline; merged 16S reads were trimmed to 400bp, followed by
163 dereplication, ASV inference, and chimera removal. The output OTU table was then used to assign
164 taxonomy using a SILVA 138 SSU database [49, 50]. The QIIME2 pipeline outputs a fasta file containing
165 all ASVs with their associated sequences, an OTU table, and a taxonomy table which are used for
166 downstream analyses. Lastly, we removed suspected contaminant ASVs (i.e. those present in sequencing
167 blanks) from both ITS and 16S datasets via the decontam v.1.8.0 package in R v.4.0.3 [44, 51].
168
169 *Statistics and other analyses*
170 All downstream analyses were performed in R v4.0.3, unless otherwise noted [44]. To make our
171 data Euclidean, we transformed it with the Hellinger Transformation (*decostand* function) prior to running
172 Principal Component Analysis (PCA, via the *rda* function) [52, 53]. PCA results were plotted using the

phyloseq v1.36 function, *plot_ordination* [54]. We used the vegan package v.2.5-7 to calculate diversity metrics and PERMANOVA [52]. For additional statistical analyses and visualization, we used the following in R v4.0.3; TITAN2 v.2.4.1 [55, 56], Venn diagram via eulerr v.6.1.0 [58], network modularity test based on the code from Whitman, *et al* using igraph v.1.2.6 [26, 59], plot visualizations via ggplot2 v.3.3.5 [60], and general data-wrangling via tidyverse v.1.3.0 [61]. The correlation network was calculated using the C++ program FastSpar v.1.0.0 [62], and visualized with the graphic program CytoScape v.3.9.1 [63]. We used Burns, *et al*'s implementation of Sloan's Community Neutral Model [16, 57] on concatenated 16S and ITS data for each plot. To investigate how neutral model fit changed over time, we divided our samples as equally as possible along the timeseries, and then rarefied samples to 6651 ASVs prior to fitting the neutral model. The fit of the neutral model did not differ substantially over time (Figure S3).

Data availability

Raw sequencing reads have been submitted to the SRA under accession XXXX. Full results of all statistics and other analyses can be found in the supplemental materials. All code that was used to process and analyze the data is publicly available here: https://github.com/TraxlerLab/BlodgettProject

RESULTS

Experimental prescribed fires

To investigate the effect of prescribed fire on soil microbial communities, we established four ten-meter transects within a mixed conifer forest at the University of California's (UC) Blodgett Forest Research Station, which is around 1360m elevation in the Sierra Nevada Mountains, CA, USA (Figure 1A). Two transects were burned ("Hi" and "Lo"), and the remaining two transects ("1c" and "2c") functioned as experimental controls that remained unburned throughout a 17 month sampling time series (Figure 1B). The two control plots haven't burned since the UC acquired the property in 1933. However, prior to that, indigenous people regularly burned the area roughly every 5 - 10 years, up until the gold rush of 1849 and subsequent rapid European colonization displaced and decimated indigenous populations across the region

199 [64]. The Lo plot was treated with low-intensity prescribed fire in 2013 and then again as part of this study
200 in October of 2018. The Hi plot experienced low-intensity prescribed burns in 2002, 2009, and 2017. In
201 January 2019, as part of this study, a slash pile (roughly 20m x 10m x 1.5m) was burned to simulate a
202 higher-intensity prescribed fire (Figure 1B). During the Lo prescribed burn, thermocouples placed 1cm
203 below the soil surface recorded a maximum temperature of 56.0 °C and returned to ambient temperature
204 less than 12 hours after the fire began (Figure 1C). Temperatures 2-6cm below the soil surface did not
205 deviate substantially from the ambient temperature during the Lo burn. During the Hi prescribed burn,
206 thermocouples placed at 3cm below the soil surface recorded a maximum temperature of 71.7 °C, and 12cm
207 below the surface reached a maximum temperature of 52.2 °C. Soil temperature after the Hi burn gradually
208 returned to ambient temperature after four days (Figure 1D). In summary, the heat from the Lo prescribed
209 burn was relatively low, shallow, and not sustained. In contrast, the heat from the Hi prescribed burn was
210 relatively high, deep, and sustained.
211
212 ***Prescribed fire alters soil microbial community composition***
213 To investigate how soil microbial communities responded over time to prescribed fire, we collected
214 triplicate soil samples from all four plots prior to burning, and then we continued collecting triplicate soil
215 samples at least once/month, every month (weather permitting) from October 2018 to February 2020. We
216 amplified and sequenced ITS2 and the V3/V4 region of 16S to analyze the soil fungal and bacterial
217 communities, respectively. Principal Component Analysis (PCA) and permutational multivariate analysis
218 of variance (PERMANOVA) found a significant difference between burned and control samples for both
219 bacterial and fungal communities ($p < 0.001$, Figure 2A). A scatterplot of fungal Principal Component (PC)
220 1 and PC2 shows three distinct sample clusters associated with either Hi prescribed burn, Lo prescribed
221 burn, or the non-burn controls (Figure 2A). In contrast, a scatterplot of bacterial PC1 and PC2 shows control
222 samples nested within an overlapping region of distinct Hi burn and Lo burn clusters (Figure 2B). For
223 fungal communities, PC1 correlates with soil pH, whereas PC2 correlates with prescribed fire treatment
224 (Figure S4). For bacterial communities, PC1 also correlates with soil pH, however none of our measured

environmental or experimental variables clearly explain the variation across PC2 (Figure S5). In contrast to the Hi prescribed burn, the Lo prescribed burn did not affect pH, which highlights that pH is not necessarily the sole determinant of post-fire microbial community assembly. Season, time since burn, average daily air temperature, and precipitation did not explain the variation between our samples (Figure S4 & S5). Prescribed fire generally did not influence diversity or richness over time, with one exception (Figure 2C & S6). After the Hi plot was burned, fungal Shannon diversity, richness, and to a lesser extent, evenness were all reduced post-fire, and remained lower than the Lo, 1c, and 2c plots throughout the sampling time series. Taken together, these results demonstrate that prescribed fire generally had a significant effect on soil microbial community composition, those effects persisted for 17 months post-fire, and higher intensity prescribed fire had a stronger effect on fungi than bacteria.

Indicator taxa associated with changes in community composition following prescribed fire

To identify significant shifts in community composition over time, we conducted a Threshold Indicator Taxa Analysis (TITAN). TITAN combines change point analysis [64, 65] and indicator species analysis [66] to find time-points where community composition changed significantly, while also highlighting dynamic taxa that were indicators of whole-community shifts [55, 56]. TITAN identified two significant change points along the time series for each of our four plots (Figure 3A and S7). The first change point in each plot is associated with indicator taxa that generally decline in abundance over time ("negative responders"), and the second change point is where indicators tend to increase over time ("positive responders") (Figure 3). The negative change points for both burned plots occurred immediately following prescribed fire, and then roughly one year later. In contrast, change points in our control plots occurred during winter months (Figure 3A). For example, plot 1c possibly experienced community shifts associated with minimum mid-winter temperatures, while 2c possibly experienced community shifts associated with the first precipitation event of the wet season (Figure S8). TITAN identified substantially more indicator taxa in burned plots (Lo = 156, Hi = 121) than in control plots (1c = 33, 2c = 73). A majority of control plot

indicators were negative responders (1c: 88%, 2c: 64%), whereas burned plot indicators were roughly evenly distributed between negative and positive responders (Figure 3B).

TITAN indicator taxa in the burned plots include many genera that have been previously described as fire-responsive (Figure 3B). We compiled a list of microbial genera from previous literature that responded positively to fire (File S2). We highlighted taxa assigned to these genera as lighter-hued sections in Figure 3B. Notably, this included the fungal genera *Pyronema*, *Geopyxis*, *Anthracobia*, *Lyophyllum,* and *Myxomphalia,* and the bacterial genera *Massilia*, *Flavobacterium*, and *Blastococcus*. Taken together, these findings demonstrate that fire led to both immediate and delayed effects on soil microbial community composition, and dynamic responders to fire included previously documented fire-associated genera.

Prescribed fire intensity drives microbial community substructure

To identify if there was significant network substructure in our community, we first calculated a correlation network (via FastSpar, which is based on Pearson correlation), and then used Clauset, *et al*'s fast greedy clustering method to test for network substructure [67]. Clauset, *et al*'s test for community substructure, or modularity, resulted in a Q-value of 0.329, and $Q > 0.3$ is considered a good indicator of network modularity [67, 68]. The network was composed of a total of 19 modules, but 98.6% of all taxa fell within the first three modules (Supplemental File S3), thus we focus on Modules 1-3. To understand factors that might underlie this modularity, we compared module assignment to relative abundances in each plot and to TITAN results (Figure 4). We set a conservative threshold to determine if a taxon was highly abundant in each sample; greater than the 95th percentile for all abundance values. 41% of all taxa in the network were consistently below the 95th percentile, thus not highly abundant (black in Figure 4A). 24% of all taxa were highly abundant in both prescribed burn and control plots, thus uninformative (gray in Figure 4A). 22% of all taxa were highly abundant in burned plots, but not control plots, and 70% of these burn-abundant taxa were assigned to network Modules 2 and 3 (red in Figure 4A). In contrast, the remaining 13% of all taxa were highly abundant in control plots, but not burned plots (blue in Figure 4A), and 77% of these control-abundant taxa were assigned to Module 1 (Figure 4A). A similar pattern was maintained

276 when the network was filtered for TITAN indicator taxa; Module 1 was enriched for indicators of the
277 control plots (44% controls, 38% Lo, 16% Hi) and Modules 2 & 3 were dominated by prescribed burn
278 indicators. Notably, indicators of the Hi prescribed burn largely fell within Module 2 (65% Hi, 17% Lo,
279 18% controls), whereas Lo prescribed burn indicators were predominantly assigned to Module 3 (71% Lo,
280 7% Hi, 22% controls). Taken together, these results point toward cohorts of microbial taxa that responded
281 positively (Modules 2 & 3), or negatively to fire (Module 1). This network substructure further
282 differentiated between taxa that were indicators for either the low-intensity burn treatment or high-intensity
283 burn treatment, indicating that the soil microbial community responded uniquely to fires of differing
284 intensities.
285
286 ***A combination of neutral and deterministic processes drive soil community assembly patterns***
287 To illuminate broad ecological processes driving community assembly, we investigated the
288 contribution of neutral and deterministic processes in structuring the soil microbial community. We fit the
289 Sloan Neutral Community Model to our data [16, 57], and then examined the taxa that fell within (neutral)
290 or outside (deterministic) the neutral prediction (Figure 5). On average 92.8% (± 0.7%) of taxa in each of
291 our plots fit the neutral prediction (Figure 5A), and the neutral model fit was roughly equivalent across all
292 plots (R^2 = 0.63 - 0.73) (Figure 5B). Importantly, the subsets of taxa identified by both TITAN and the
293 correlation network analysis were enriched for taxa that fell outside the neutral prediction (Figure 5A).
294 Roughly half of all taxa identified as indicators by TITAN were non-neutral, and 54% of taxa in network
295 modules 1 - 3 were also nonneutral. Notably, Module 2 was enriched for taxa that were non-neutral in the
296 Hi burn plot, whereas Module 3 was enriched for non-neutral taxa in the Lo burn plot. Several previously
297 described fire-responsive taxa fell outside the neutral prediction in both burned plots, which are highlighted
298 in Figure 5B. Lastly, Sloan's Neutral Community Model estimates the rate of dispersal, or migration (m)
299 into the community. This migration value in all plots was close to zero ($m < 0.01$), indicating that dispersal
300 likely has very limited influence on community structure in either control or burned plots. Together these
301 data demonstrate that a majority of taxa in our samples are present due to stochastic, or neutral processes.

However, the neutral model did not predict the presence of the majority of indicator taxa that dynamically responded to fire, implying that their presence was likely the result of deterministic processes, i.e. selection.

Pyrophilous genera associated with prescribed fire

We leveraged the results of TITAN, neutral model fit, and the correlation network analyses to independently identify pyrophilous taxa within our data (Figure 6). Figure 6A-C details our methodology for identifying pyrophilous taxa. Briefly, we subset the correlation network for the 96 taxa that were unique to burned plots as TITAN indicators and/or non-neutral (Figure 6A&B), and then further filtered this list for taxa that were highly abundant only in burned plots (Figure 6C). These filtering steps resulted in nine unique genera, which we consider to be pyrophilous: the fungi *Pyronema*, *Geopyxis*, *Lyophyllum*, *Myxomphalia*, *Rhodosporidiobolus*, and the bacteria *Massilia*, *Bacillus*, *Flavobacterium*, and *Cellvibrio*. These taxa are highlighted in the network in Figure 6B, and we illustrate their average normalized relative abundance over time in Figure 6D. All pyrophilous genera except *Cellvibrio* were assigned to network Module 2. *Cellvibrio* fell within Module 3, along with one of three *Flavobacterium* ASVs (Figure 6B). The average abundance of the pyrophilous genera over time in both the Lo burn and control plots generally mirrors precipitation events (Figure S8), however abundances were substantially higher after burning and decreasing over time. *Pyronema* dominated immediately after the Lo prescribed burn prior to any precipitation (the Lo plot was burned on 16 Oct 2018 and the first rain was on 20 Nov 2018). Following the start of the rainy season, *Pyronema* and all the pyrophilous bacteria peaked in abundance (Figure 6D). The Hi plot was treated with prescribed fire during a mid-winter dry period, and precipitation occurred one day after starting the fire. *Geopyxis* peaked in abundance immediately after the Hi burn (Figure 6D). *Lyophyllum*, *Bacillus*, and *Massilia* also experienced a peak in abundance at the first sampling time point following the Hi prescribed burn. In contrast to the Lo burn, *Pyronema* peaked in abundance three months after the Hi burn, along with *Rhodosporidiobolus, Flavobacterium,* and *Massilia.* All nine pyrophiles increased dramatically in abundance following the Hi prescribed burn. In contrast, in the Lo plot, *Lyophyllum* and *Rhodosporidiobolus* were not abundant at any time point. In conclusion, this combined

328 analysis independently identified nine pyrophilous genera that responded strongly and positively, likely
329 through deterministic processes associated with prescribed fire at Blodgett Forest.
330
331 **DISCUSSION**
332 As the incidence of wildfire increases with ongoing climate change, strategies for mitigating their
333 impact, including prescribed burns, are becoming increasingly relevant. Here, we sought to understand the
334 impact of prescribed fire on soil fungal and bacterial communities, and the ecological processes that
335 influence post-fire microbial community assembly. We undertook extensive time-course sampling of two
336 prescribed burn plots, one which experienced a low intensity fire, and a second that experienced a higher
337 intensity fire. We found that fire significantly altered both the fungal and bacterial communities in the
338 burned plots, as compared to unburned control plots. Using a series of downstream analyses, we conclude
339 that, while a large portion of the post-prescribed burn community is likely assembled via neutral processes,
340 a subcommunity that includes pyrophilous organisms likely arises through deterministic processes. A
341 number of other studies have begun to paint a picture of post-fire microbial community structure [12, 22,
342 24, 26, 31, 69–73], and this work further builds on those by identifying members of the subcommunity that
343 deterministically respond to fire. In doing so, this work lays the foundation for building a process-driven
344 understanding of microbial community assembly in the context of the classical disturbance regime of fire.
345 Neutral processes such as passive dispersal and ecological drift have been shown to be important
346 during the colonization of unoccupied environments, and a recently burned landscape may seem,
347 superficially, like such an environment. However, many organisms survive below the soil surface even
348 during intense wildfires [12], and organismal survival becomes more likely with decreasing fire intensity.
349 This notion is consistent with our data showing that lower-intensity prescribed fires had a minimal impact
350 on richness (Figure 2C-D). We also found that the majority (~93%) of the soil microbial community at
351 Blodgett Forest could be accounted for by a model of neutral assembly (regardless of fire occurrence).
352 Thus, the community structure in our burned plots likely reflects a combination of; (1) the legacy of
353 neutrality in the soil microbial communities that was present prior to fire, (2) *de novo* community assembly

354 through neutral processes, and (3) selection of a subcommunity of microbes adapted to postfire
355 environments.

356 To identify members of the fire-responsive subcommunity, we used TITAN and a correlation
357 network analysis, in conjunction with a neutral model. TITAN highlighted individual indicator taxa whose
358 abundances were dynamic across time, while correlation network analysis identified sub-groups of taxa
359 whose members were linked through correlations in abundance, irrespective of time. Importantly, the
360 subcommunity identified by the combined correlation analysis and TITAN was enriched for non-neutral
361 taxa (Figure 5A), indicating that deterministic processes likely played an important role in the assembly of
362 this fire-responsive subcommunity. Fire is a dramatic selective force that has a myriad of effects on soil,
363 such as direct heating during the fire and enduring post-fire effects including increased pH, increased
364 hydrophobicity, decreased bioavailability of nutrients (especially nitrogen), and the deposition of a layer of
365 PyOM and mineral ash. Our data do not allow us to directly distinguish between these possible selective
366 forces associated with prescribed fire. However, it is notable that in our Lo burned plot we did not observe
367 any significant changes in pH, and there was little-to-no effect of heat below the soil surface (Figure 1C,
368 S4 & S5), yet we still observed a significant effect on community composition. Thus, we hypothesize that
369 factors beyond temperature and pH, such as deposition of PyOM, may underlie assembly of the fire-
370 responsive sub-community following low-intensity fire. Further investigation will be required to test this
371 hypothesis *in situ*.

372 Taxa that fall above the neutral prediction in Sloan's Neutral Community Model are found more
373 frequently than would be predicted by their abundance in the metacommunity. Conversely, taxa that fall
374 below are highly abundant in fewer samples than would be expected, resulting from a patchy distribution
375 across samples. Burns, *et al* suggested that taxa above the neutral prediction are being selected for, whereas
376 taxa below may be seen as 'invasive', or are dispersal limited, or are selected against. It's notable that most
377 taxa that we identify as pyrophilous fell below the neutral partition in our burned plots (Figure 5B),
378 indicating that they were found at high abundance with relatively low frequency. Such a patchy distribution
379 may be explained by the fact that the effects of fire across a landscape result in a spatially heterogeneous

mosaic [74, 75]. For example, individual soil patches experience varied levels of perturbation from irregular heating, as well as non-uniform deposition of PyOM and changes in pH. Alternatively, patchy distributions of locally abundant taxa can arise as a result of interference competition that leads to spatial segregation of competing organisms [76, 77], although more study will be required to link this possibility to taxa that fall below neutral model predictions.

While there are numerous previous descriptions of pyrophilous taxa (File S2), we add to this body of work by using multiple analyses to independently identify pyrophilous taxa in post-prescribed burn environments. Specifically, we included taxa that; (1) were dynamic over time in burned plots according to TITAN, (2) showed strong correlation patterns with other community members, (3) fell outside the neutral expectation in burned plots, and (4) were only highly abundant in burned plots (Figure 6A-C). Only nine genera passed through this stringent filtering process, six of which have been previously reported as pyrophilous (*Pyronema, Myxomphalia, Lyophyllum, Geopyxis, Massilia*, and *Flavobacterium*). The three genera that are currently absent from other pyrophile literature are *Bacillus, Cellvibrio,* and *Rhodosporidiobolus*. *Bacillus* (Firmicutes) are well-known, ubiquitous soil bacteria that form remarkably resistant spores, which could be important for surviving the heat of intense fires. Beyond survival, we note that several species of *Bacillus* are known to degrade polycyclic aromatic hydrocarbons, which may be relevant in the consumption of PyOM [78, 79]. *Cellvibrio* (Gammaproteobacteria) are also common soil inhabitants that have recently drawn biotechnology interest for their production of xylanases and other carbohydrate active enzymes [80], and some isolates have demonstrated the ability to fix nitrogen [81], which could be critically important for life in nitrogen-depleted post-fire soils [82]. *Rhodosporidiobolus* is a red yeast in the Pucciniomycotina (Basidiomycota) that was first described in 2015 [83] and has since been found to increase in abundance after biochar addition to tea orchard soil [84], and demonstrated a robust ability to degrade lignin and other aromatic compounds [85]. These examples point toward the notion that *Rhodosporidiobolus* may be able to utilize the PyOM component of a recently burned environment, similar to *Pyronema domesticum* [86].

All microbial communities are assembled through some combination of the deterministic process of ecological selection (encompassing environmental filtering and biotic interactions) and the stochastic processes of passive dispersal, ecological drift, and mutation/speciation. Here we used parallel analyses to identify taxa that were temporally dynamic, showed patterns of co-occurrence, and whose presence was likely attributable to deterministic processes. In delineating this pyrophilous subcommunity, this work lays the foundation for future investigations into the mechanisms that drive pyrophilous community assembly in post-fire environments. Furthermore, we speculate that interactions among members of this sub-community may impact the degradation and reintegration of pyrolyzed organic matter in areas under pressure from increasingly frequent wildfires. Finally, this work sets the stage for understanding the role of this subcommunity in stimulating the recovery of the broader community of micro- and macro-organisms, while also providing a starting point for future studies aimed at harnessing deterministic interventions to enhance community resilience to fire.

ACKNOWLEDGEMENTS

This research would not have been possible without the incredible support of Ariel Thomson Roughton, Robert York, Amy Mason, and everyone at Blodgett Forest Research Station. We are also grateful for Peter Wyrsch, Thea Whitman, and Luis Cantu Morin for many fruitful conversations. This research used the Savio computational cluster resource provided by the Berkeley Research Computing program at the University of California, Berkeley (supported by the UC Berkeley Chancellor, Vice Chancellor for Research, and Chief Information Officer). The sequencing was carried out at the DNA Technologies and Expression Analysis Cores at the UC Davis Genome Center, supported by NIH Shared Instrumentation Grant 1S10OD010786-01. This research was supported by the DOE Office of Science and Office of Biological and Environmental Research (BER); grant no. DE-SC0020351 to MT.

REFERENCES

1. Flannigan MD, Krawchuk MA, de Groot WJ, Wotton BM, Gowman LM. Implications of changing climate for global wildland fire. *Int J Wildland Fire* 2009; **18**: 483.
2. Doerr SH, Santín C. Global trends in wildfire and its impacts: perceptions versus realities in a changing world. *Phil Trans R Soc B* 2016; **371**: 20150345.
3. Mueller SE, Thode AE, Margolis EQ, Yocom LL, Young JD, Iniguez JM. Climate relationships with increasing wildfire in the southwestern US from 1984 to 2015. *Forest Ecology and Management* 2020; **460**: 117861.
4. Giglio L, Randerson JT, van der Werf GR. Analysis of daily, monthly, and annual burned area using the fourth-generation global fire emissions database (GFED4): ANALYSIS OF BURNED AREA. *J Geophys Res Biogeosci* 2013; **118**: 317–328.
5. Bird MI, Wynn JG, Saiz G, Wurster CM, McBeath A. The Pyrogenic Carbon Cycle. *Annu Rev Earth Planet Sci* 2015; **43**: 273–298.
6. Bowman DMJS, Balch JK, Artaxo P, Bond WJ, Carlson JM, Cochrane MA, et al. Fire in the Earth System. *Science* 2009; **324**: 481–484.
7. Pellegrini AFA, Ahlström A, Hobbie SE, Reich PB, Nieradzik LP, Staver AC, et al. Fire frequency drives decadal changes in soil carbon and nitrogen and ecosystem productivity. *Nature* 2018; **553**: 194–198.
8. Agee JK, Skinner CN. Basic principles of forest fuel reduction treatments. *Forest Ecology and Management* 2005; **211**: 83–96.
9. North MP, York RA, Collins BM, Hurteau MD, Jones GM, Knapp EE, et al. Pyrosilviculture Needed for Landscape Resilience of Dry Western United States Forests. *Journal of Forestry* 2021; **119**: 520–544.
10. Ryan KC, Knapp EE, Varner JM. Prescribed fire in North American forests and woodlands: history, current practice, and challenges. *Frontiers in Ecology and the Environment* 2013; **11**.

11. Kramer A, Jones GM, Whitmore SA, Keane JJ, Atuo FA, Dotters BP, et al. California spotted owl habitat selection in a fire-managed landscape suggests conservation benefit of restoring historical fire regimes. *Forest Ecology and Management* 2021; **479**: 118576.
12. Certini G, Moya D, Lucas-Borja ME, Mastrolonardo G. The impact of fire on soil-dwelling biota: A review. *Forest Ecology and Management* 2021; **488**: 118989.
13. Brockway DG, Lewis CE. Long-term effects of dormant-season prescribed fire on plant community diversity, structure and productivity in a longleaf pine wiregrass ecosystem. *Forest Ecology and Management* 1997; **96**: 167–183.
14. Woolet J, Whitman T. Pyrogenic organic matter effects on soil bacterial community composition. *Soil Biology and Biochemistry* 2020; **141**: 107678.
15. Hanson CA, Fuhrman JA, Horner-Devine MC, Martiny JBH. Beyond biogeographic patterns: processes shaping the microbial landscape. *Nature Reviews Microbiology* 2012; **10**: 497–506.
16. Burns AR, Stephens WZ, Stagaman K, Wong S, Rawls JF, Guillemin K, et al. Contribution of neutral processes to the assembly of gut microbial communities in the zebrafish over host development. *ISME J* 2016; **10**: 655–664.
17. Ferrenberg S, O'Neill SP, Knelman JE, Todd B, Duggan S, Bradley D, et al. Changes in assembly processes in soil bacterial communities following a wildfire disturbance. *The ISME Journal* 2013; **7**: 1102–1111.
18. Meiners SJ, Cadotte MW, Fridley JD, Pickett STA, Walker LR. Is successional research nearing its climax? New approaches for understanding dynamic communities. *Funct Ecol* 2015; **29**: 154–164.
19. Bruns TD, Chung JA, Carver AA, Glassman SI. A simple pyrocosm for studying soil microbial response to fire reveals a rapid, massive response by Pyronema species. *PLoS ONE* 2020; **15**: e0222691.
20. Holden SR, Treseder KK. A meta-analysis of soil microbial biomass responses to forest disturbances. *Frontiers in Microbiology* 2013; **4**: 1–17.

481 21. Pressler Y, Moore JC, Cotrufo MF. Belowground community responses to fire: meta-analysis reveals
482 contrasting responses of soil microorganisms and mesofauna. *Oikos* 2018; **128**: 309–327.
483 22. Dooley SR, Treseder KK. The effect of fire on microbial biomass: a meta-analysis of field studies.
484 *Biogeochemistry* 2012; **109**: 49–61.
485 23. Glassman SI, Levine CR, DiRocco AM, Battles JJ, Bruns TD. Ectomycorrhizal fungal spore bank
486 recovery after a severe forest fire: some like it hot. *The ISME Journal* 2016; **10**: 1228–1239.
487 24. Day NJ, Dunfield KE, Johnstone JF, Mack MC, Turetsky MR, Walker XJ, et al. Wildfire severity
488 reduces richness and alters composition of soil fungal communities in boreal forests of western
489 Canada. *Global Change Biology* 2019; gcb.14641.
490 25. Weber CF, Lockhart JS, Charaska E, Aho K, Lohse KA. Bacterial composition of soils in ponderosa
491 pine and mixed conifer forests exposed to different wildfire burn severity. *Soil Biology and*
492 *Biochemistry* 2014; **69**: 242–250.
493 26. Whitman T, Whitman E, Woolet J, Flannigan MD, Thompson DK, Parisien M-A. Soil bacterial and
494 fungal response to wildfires in the Canadian boreal forest across a burn severity gradient. *Soil*
495 *Biology and Biochemistry* 2019; **138**: 107571.
496 27. Xiang X, Shi Y, Yang J, Kong J, Lin X, Zhang H, et al. Rapid recovery of soil bacterial communities
497 after wildfire in a Chinese boreal forest. *Scientific Reports* 2014; **4**: 1–8.
498 28. Seaver FJ. Studies in pyrophilous fungi: I. The occurrence and cultivation of Pyronema. *Mycologia*
499 1909; **1**: 131–139.
500 29. Lisiewska M. Macrofungi on special substrates. In: Winterhoff W (ed). *Fungi in vegetation science*.
501 1992. Springer Netherlands, Dordrecht, pp 151–182.
502 30. Petersen PM. Danish Fireplace Fungi, 3rd ed. 1970. Dansk Botanisk Arkiv.
503 31. Mino L, Kolp MR, Fox S, Reazin C, Zeglin L, Jumpponen A. Watershed and fire severity are
504 stronger determinants of soil chemistry and microbiomes than within-watershed woody
505 encroachment in a tallgrass prairie system. *FEMS Microbiology Ecology* 2021; **97**: fiab154.

506 32. Qin Q, Liu Y. Changes in microbial communities at different soil depths through the first rainy
507 season following severe wildfire in North China artificial Pinus tabulaeformis forest. *Journal of*
508 *Environmental Management* 2021; **280**: 111865.
509 33. Hughes KW, Matheny PB, Miller AN, Petersen RH, Iturriaga TM, Johnson KD, et al. Pyrophilous
510 fungi detected after wildfires in the Great Smoky Mountains National Park expand known species
511 ranges and biodiversity estimates. *Mycologia* 2020; **112**: 677–698.
512 34. Livne-Luzon S, Shemesh H, Osem Y, Carmel Y, Migael H, Avidan Y, et al. High resilience of the
513 mycorrhizal community to prescribed seasonal burnings in eastern Mediterranean woodlands.
514 *Mycorrhiza* 2021; **31**: 203–216.
515 35. Adamczyk JJ, Kruk A, Penczak T, Minter D. Factors shaping communities of pyrophilous
516 macrofungi in microhabitats destroyed by illegal campfires. *Fungal Biology* 2012; **116**: 995–1002.
517 36. Raudabaugh DB, Matheny PB, Hughes KW, Iturriaga T, Sargent M, Miller AN. Where are they
518 hiding? Testing the body snatchers hypothesis in pyrophilous fungi. *Fungal Ecology* 2020; **43**: 1–10.
519 37. Day NJ, Cumming SG, Dunfield KE, Johnstone JF, Mack MC, Reid KA, et al. Identifying Functional
520 Impacts of Heat-Resistant Fungi on Boreal Forest Recovery After Wildfire. *Front For Glob Change*
521 2020; **3**: 68.
522 38. Li W, Niu S, Liu X, Wang J. Short-term response of the soil bacterial community to differing wildfire
523 severity in Pinus tabulaeformis stands. *Sci Rep* 2019; **9**: 1148.
524 39. Simmons T, Caddell DF, Deng S, Coleman-Derr D. Exploring the Root Microbiome: Extracting
525 Bacterial Community Data from the Soil, Rhizosphere, and Root Endosphere. *JoVE* 2018; 57561.
526 40. Gao C, Montoya L, Xu L, Madera M, Hollingsworth J, Purdom E, et al. Strong succession in
527 arbuscular mycorrhizal fungal communities. *The ISME Journal* 2018.
528 41. Taylor DL, Walters WA, Lennon NJ, Bochicchio J, Krohn A, Caporaso JG, et al. Accurate
529 Estimation of Fungal Diversity and Abundance through Improved Lineage-Specific Primers
530 Optimized for Illumina Amplicon Sequencing. *Applied and Environmental Microbiology* 2016; **82**:
531 7217–7226.

42. Palmer JM, Jusino MA, Banik MT, Lindner DL. Non-biological synthetic spike-in controls and the AMPtk software pipeline improve mycobiome data. *PeerJ* 2018; **6**: e4925.

43. Callahan BJ, McMurdie PJ, Rosen MJ, Han AW, Johnson AJA, Holmes SP. DADA2: High-resolution sample inference from Illumina amplicon data. *Nat Methods* 2016; **13**: 581–583.

44. R Core Team. R: A language and environment for statistical computing. 2020. R Foundation for Statistical Computing, Vienna, Austria.

45. Nilsson RH, Larsson K-H, Taylor AFS, Bengtsson-Palme J, Jeppesen TS, Schigel D, et al. The UNITE database for molecular identification of fungi: handling dark taxa and parallel taxonomic classifications. *Nucleic Acids Research* 2019; **47**: D259–D264.

46. Nguyen NH, Song Z, Bates ST, Branco S, Tedersoo L, Menke J, et al. FUNGuild: An open annotation tool for parsing fungal community datasets by ecological guild. *Fungal Ecology* 2016; **20**: 241–248.

47. Estaki M, Jiang L, Bokulich NA, McDonald D, González A, Kosciolek T, et al. QIIME 2 Enables Comprehensive End-to-End Analysis of Diverse Microbiome Data and Comparative Studies with Publicly Available Data. *Current Protocols in Bioinformatics* 2020; **70**.

48. Martin M. Cutadapt removes adapter sequences from high-throughput sequencing reads. *EMBnet.journal* 2011; **17**: 10–12.

49. Yilmaz P, Parfrey LW, Yarza P, Gerken J, Pruesse E, Quast C, et al. The SILVA and "All-species Living Tree Project (LTP)" taxonomic frameworks. *Nucl Acids Res* 2014; **42**: D643–D648.

50. Quast C, Pruesse E, Yilmaz P, Gerken J, Schweer T, Yarza P, et al. The SILVA ribosomal RNA gene database project: improved data processing and web-based tools. *Nucleic Acids Research* 2012; **41**: D590–D596.

51. Davis NM, Proctor DM, Holmes SP, Relman DA, Callahan BJ. Simple statistical identification and removal of contaminant sequences in marker-gene and metagenomics data. *Microbiome* 2018; **6**: 226.

52. Oksanen J, Blanchet F. G, Friendly M, Kindt R, Legendre P, McGlinn D, et al. vegan: community ecology package. R package version 2.5-7. 2020.

53. Borcard D, Gillet F, Legendre P. Numerical Ecology with R. 2018. Springer International Publishing, Cham.

54. McMurdie PJ, Holmes S. phyloseq: An R Package for Reproducible Interactive Analysis and Graphics of Microbiome Census Data. *PLoS ONE* 2013; **8**: e61217.

55. Baker ME, King RS. A new method for detecting and interpreting biodiversity and ecological community thresholds: *Threshold Indicator Taxa ANalysis (TITAN)*. *Methods in Ecology and Evolution* 2010; **1**: 25–37.

56. Baker ME, King RS. Of TITAN and straw men: an appeal for greater understanding of community data. *Freshwater Science* 2013; **32**: 489–506.

57. Larsson J. eulerr: Area-Proportional Euler and Venn Diagrams with Ellipses. 2021.

58. Csardi G, Nepusz T. The igraph software package for complex network research. *InterJournal* 2006; **Complex Systems**: 1695.

59. Wickham H. ggplot2: Elegant Graphics for Data Analysis. 2009. Springer-Verlag New York.

60. Wickham H, Averick M, Bryan J, Chang W, McGowan L, François R, et al. Welcome to the Tidyverse. *JOSS* 2019; **4**: 1686.

61. Watts SC, Ritchie SC, Inouye M, Holt KE. FastSpar: rapid and scalable correlation estimation for compositional data. *Bioinformatics* 2019; **35**: 1064–1066.

62. Shannon P, Markiel A, Ozier O, Baliga NS, Wang JT, Ramage D, et al. Cytoscape: A Software Environment for Integrated Models of Biomolecular Interaction Networks. *Genome Res* 2003; **13**: 2498–2504.

63. Sloan WT, Lunn M, Woodcock S, Head IM, Nee S, Curtis TP. Quantifying the roles of immigration and chance in shaping prokaryote community structure. *Environ Microbiol* 2006; **8**: 732–740.

64. Taylor AH, Trouet V, Skinner CN, Stephens S. Socioecological transitions trigger fire regime shifts and modulate fire–climate interactions in the Sierra Nevada, USA, 1600–2015 CE. *Proc Natl Acad Sci USA* 2016; **113**: 13684–13689.

583 65. King RS, Richardson CJ. Integrating Bioassessment and Ecological Risk Assessment: An Approach
584 to Developing Numerical Water-Quality Criteria. *Environmental Management* 2003; **31**: 795–809.
585 66. Qian SS, King RS, Richardson CJ. Two statistical methods for the detection of environmental
586 thresholds. *Ecological Modelling* 2003; **166**: 87–97.
587 67. Dufrêne M, Legendre P. Species assemblages and indicator species: the need for a flexible
588 asymmetrical approach. *Ecological Monographs* 1997; **67**: 345–366.
589 68. Clauset A, Newman MEJ, Moore C. Finding community structure in very large networks. *Phys Rev E*
590 2004; **70**: 066111.
591 69. Newman MEJ. Modularity and community structure in networks. *Proceedings of the National*
592 *Academy of Sciences* 2006; **103**: 8577–8582.
593 70. Pérez-Valera E, Verdú M, Navarro-Cano JA, Goberna M. Resilience to fire of phylogenetic diversity
594 across biological domains. *Molecular Ecology* 2018; **27**: 2896–2908.
595 71. Semenova-Nelsen TA, Platt WJ, Patterson TR, Huffman J, Sikes BA. Frequent fire reorganizes
596 fungal communities and slows decomposition across a heterogeneous pine savanna landscape. *New*
597 *Phytol* 2019; nph.16096.
598 72. Dove NC, Klingeman DM, Carrell AA, Cregger MA, Schadt CW. Fire alters plant microbiome
599 assembly patterns: integrating the plant and soil microbial response to disturbance. *New Phytol* 2021;
600 nph.17248.
601 73. Cutler NA, Arróniz-Crespo M, Street LE, Jones DL, Chaput DL, DeLuca TH. Long-Term Recovery
602 of Microbial Communities in the Boreal Bryosphere Following Fire Disturbance. *Microbial Ecology*
603 2017; **73**: 75–90.
604 74. Fox S, Sikes BA, Brown SP, Cripps CL, Glassman SI, Hughes K, et al. Fire as a driver of fungal
605 diversity — A synthesis of current knowledge. *Mycologia* 2022; 1–27.
606 75. Meddens AJH, Kolden CA, Lutz JA, Smith AMS, Cansler CA, Abatzoglou JT, et al. Fire Refugia:
607 What Are They, and Why Do They Matter for Global Change? *BioScience* 2018.

608 76. Krawchuk MA, Meigs GW, Cartwright JM, Coop JD, Davis R, Holz A, et al. Disturbance refugia
609 within mosaics of forest fire, drought, and insect outbreaks. *Front Ecol Environ* 2020; **18**: 235–244.
610 77. Rendueles O, Amherd M, Velicer GJ. Positively Frequency-Dependent Interference Competition
611 Maintains Diversity and Pervades a Natural Population of Cooperative Microbes. *Current Biology*
612 2015; **25**: 1673–1681.
613 78. Abrudan MI, Smakman F, Grimbergen AJ, Westhoff S, Miller EL, van Wezel GP, et al. Socially
614 mediated induction and suppression of antibiosis during bacterial coexistence. *Proc Natl Acad Sci*
615 *USA* 2015; **112**: 11054–11059.
616 79. Hunter R, Ekunwe S, Dodor D, Hwang H-M, Ekunwe L. Bacillus subtilis is a Potential Degrader of
617 Pyrene and Benzo[a]pyrene. *IJERPH* 2005; **2**: 267–271.
618 80. Sultana OF, Lee S, Seo H, Mahmud HA, Kim S, Seo A, et al. Biodegradation and Removal of PAHs
619 by *Bacillus velezensis* Isolated from Fermented Food. *J Microbiol Biotechnol* 2021; **31**: 999–1010.
620 81. Attia MA, Nelson CE, Offen WA, Jain N, Davies GJ, Gardner JG, et al. In vitro and in vivo
621 characterization of three Cellvibrio japonicus glycoside hydrolase family 5 members reveals potent
622 xyloglucan backbone-cleaving functions. *Biotechnol Biofuels* 2018; **11**: 45.
623 82. Suarez C, Ratering S, Kramer I, Schnell S. Cellvibrio diazotrophicus sp. nov., a nitrogen-fixing
624 bacteria isolated from the rhizosphere of salt meadow plants and emended description of the genus
625 Cellvibrio. *International Journal of Systematic and Evolutionary Microbiology* 2014; **64**: 481–486.
626 83. Wan S, Hui D, Luo Y. Fire effects on nitrogen pools and dynamics in terrestrial ecosystems: a meta-
627 analysis. *Ecological Applications* 2001; **11**: 1349–1365.
628 84. Wang Q-M, Yurkov AM, Göker M, Lumbsch HT, Leavitt SD, Groenewald M, et al. Phylogenetic
629 classification of yeasts and related taxa within *Pucciniomycotina*. *Studies in Mycology* 2015; **81**:
630 149–189.
631 85. Yang W, Li C, Wang S, Zhou B, Mao Y, Rensing C, et al. Influence of biochar and biochar-based
632 fertilizer on yield, quality of tea and microbial community in an acid tea orchard soil. *Applied Soil*
633 *Ecology* 2021; **166**: 104005.

86. Margesin R, Ludwikowski TM, Kutzner A, Wagner AO. Low-Temperature Biodegradation of Lignin-Derived Aromatic Model Monomers by the Cold-Adapted Yeast Rhodosporidiobolus colostri Isolated from Alpine Forest Soil. *Microorganisms* 2022; **10**: 515.

87. Fischer MS, Stark FG, Berry TD, Zeba N, Whitman T, Traxler MF. Pyrolyzed Substrates Induce Aromatic Compound Metabolism in the Post-fire Fungus, Pyronema domesticum. *Front Microbiol* 2021; **12**: 729289.

650 **FIGURE LEGENDS**

651

652 **Figure 1: Site description and soil temperature during experimental burns.**

653 **(A)** Topographic map showing the location of each transect at Blodgett Experimental Forest. Brown
654 topographic lines denote elevation in meters, solid black lines indicate paved roads, dashed black lines
655 indicate dirt roads, purple line indicates the Blodgett Forest property boundary, and blue lines are streams.
656 "1c" = no burn control #1, "2c" = no burn control #2, "Lo" = low-intensity burn, "Hi" = high-intensity
657 burn. **(B)** Photos each transect. Purple dashed line highlights the location of each 10m transect. Photos of
658 1c and Lo were taken one week after fire in October 2018. The 2c and Hi transect photos we taken the same
659 day as the start of the fire in January 2019. **(C & D)** Soil temperature measured every 15 minutes starting
660 a few hours prior to each experimental burn near the Lo transect (C), and Hi transect (D). Two
661 thermocouples were placed at each depth, and temperature measurements continued for at least four days,
662 the x-axis is divided into 12-hour increments.

663

664 **Figure 2. Fire alters soil microbial community structure**

665 **(A & B)** Principal Component Analysis (PCA) on Hellinger-transformed ITS (A) & 16S (B) amplicon
666 community sequencing data. Axes are the two Principal Components (PC) that explained the most variation
667 in the data (% variation noted on each axis). Ellipses = 95% confidence interval. PERMANOVA $p < 0.001$
668 for burned vs. unburned in both ITS and 16S. **(C & D)** Community richness over time for ITS (C) and 16S
669 (D) data. Points are individual samples, and the data for each plot are summarized by fitting a local
670 polynomial regression line. The shaded area around each line indicates a 95% confidence interval.

671

672 **Figure 3. Shifts in microbial community composition associated with fire and TITAN identified a**
673 **greater number known fire-responsive taxa as indicators in fire-treated plots**

674 **(A)** Total number of indicator taxa identified by TITAN as either positively or negatively responsive, and
675 the corresponding change point date for each plot. Dashed vertical line and flame emoji denote the time-

676 point at which burned plots were burned. **(B)** Proportion of known fire-responsive taxa within positive
677 (red) or negative (blue) response groups for Control 1, Control 2, Hi-burn, and Lo-burn plots.
678
679 **Figure 4. Correlation network clusters taxa by fire treatment**
680 Correlation network arranged into modules defined by greedy clustering [67], which identified a total of 19
681 modules, modules with less than 10 nodes were excluded. Nodes are taxa, and lines represent a significant
682 correlation between taxa ($p < 0.01$, FastSpar). Purple line = positive correlation, black line = negative
683 correlation. **(A)** Complete network. For clarity, only edges and nodes with correlations > 0.3 are shown.
684 Node colors indicate the treatment(s) in which the taxon was highly abundant; red = burn, cyan = control,
685 grey = both burn and control, and black indicates taxa that were consistently in low abundance (< 95th
686 percentile) and subsequently excluded from the presence/absence analysis. **(B)** Subset of the complete
687 network showing the 335 taxa that were identified as significant indicators by TITAN. All significant
688 correlation values are shown ($p < 0.01$), and line width is proportional to the correlation value. Node colors
689 indicate in which plot the taxon was identified by TITAN as an indicator, briefly, cool colors represent
690 control plots and warm colors represent burned plots.
691
692 **Figure 5. A combination of neutral and deterministic processes drive community assembly patterns**
693 **(A)** Stacked bar-plots illustrating the number of taxa that fell within, above, or below the neutral model in
694 each plot, for all taxa and subsets of taxa based on TITAN or the correlation network analysis. **(B)** The
695 Sloan Neutral Community Model fit to ITS and 16S data in each plot. The neutral prediction is a solid dark-
696 grey line, with 95% confidence interval around indicated with dashed dark-grey lines. Taxa that fall within
697 this 95% confidence interval are colored grey. Taxa that fall outside the neutral predicted are colored either
698 orange (above) or purple (below). Taxa that were found to be indicators via TITAN are circled in black,
699 and of these indicators, those that have been previously described as fire-responsive are circled in either
700 green (fungi) or cyan (bacteria). Fire-responsive TITAN indicators that fell outside the neurtral prediction
701 are named. R^2 quantifies how well the neutral model fit the data, and m is the estimated migration rate.

Figure 6. Identification of pyrophilous genera at Blodgett Forest, and their dynamics over time. **(A)** Venn Diagram showing the number of taxa that were either identified as indicators by TITAN or fell outside the neutral prediction. **(B)** Filtered version of the correlation network depicted in Figure 4. This network was filtered for the 96 ASVs that were unique to burns in A. Pyrophilous taxa are highlighted and labeled (green outline = fungus, blue outline = bacteria). Lines thickness it proportional to the correlation value (purple = positive, black = negative). Node colors indicate the plot in which the taxon was an indicator. **(C)** Diagram describing the criteria for defining pyrophilous genera in our dataset. **(D)** Relative abundance of pyrophilous genera over time in each plot. Dashed vertical line and flame emoji denote the time-point at which burned plots were burned. Each point represents the average abundance of all ASVs for each genus at each timepoint, and average abundances were normalized to the maximum average abundance for each genus.

Figure 1

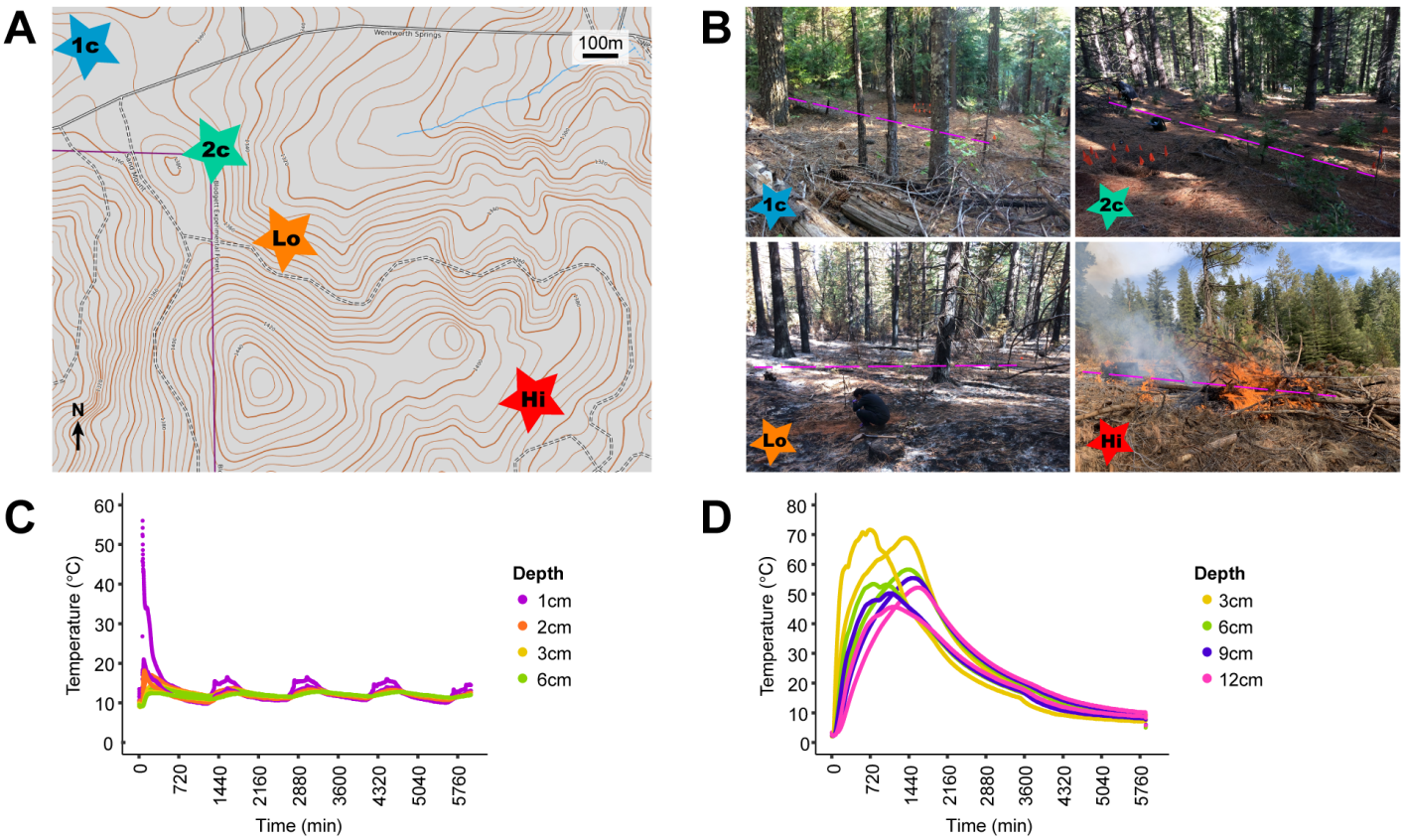

Figure 2

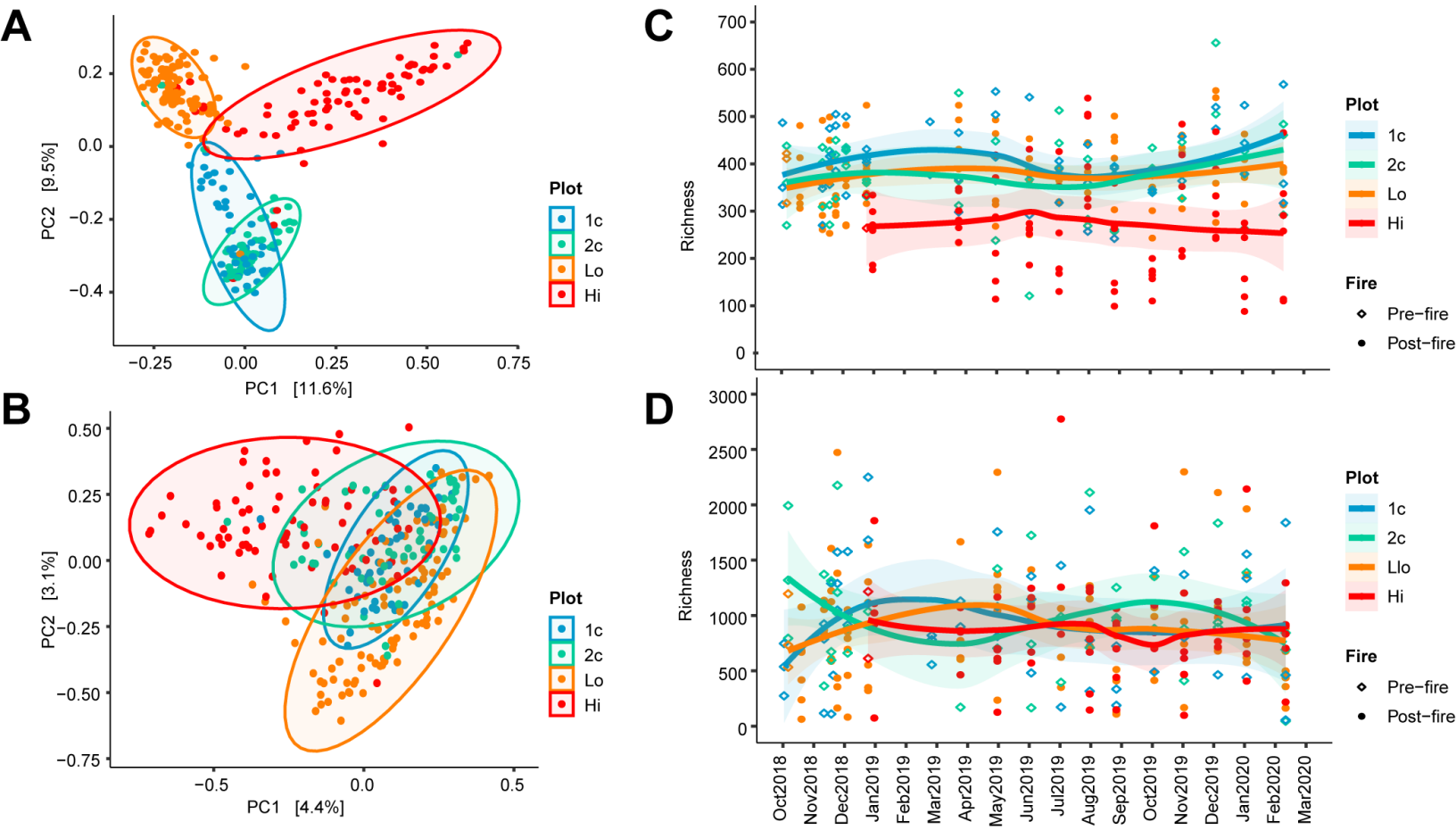

Figure 3

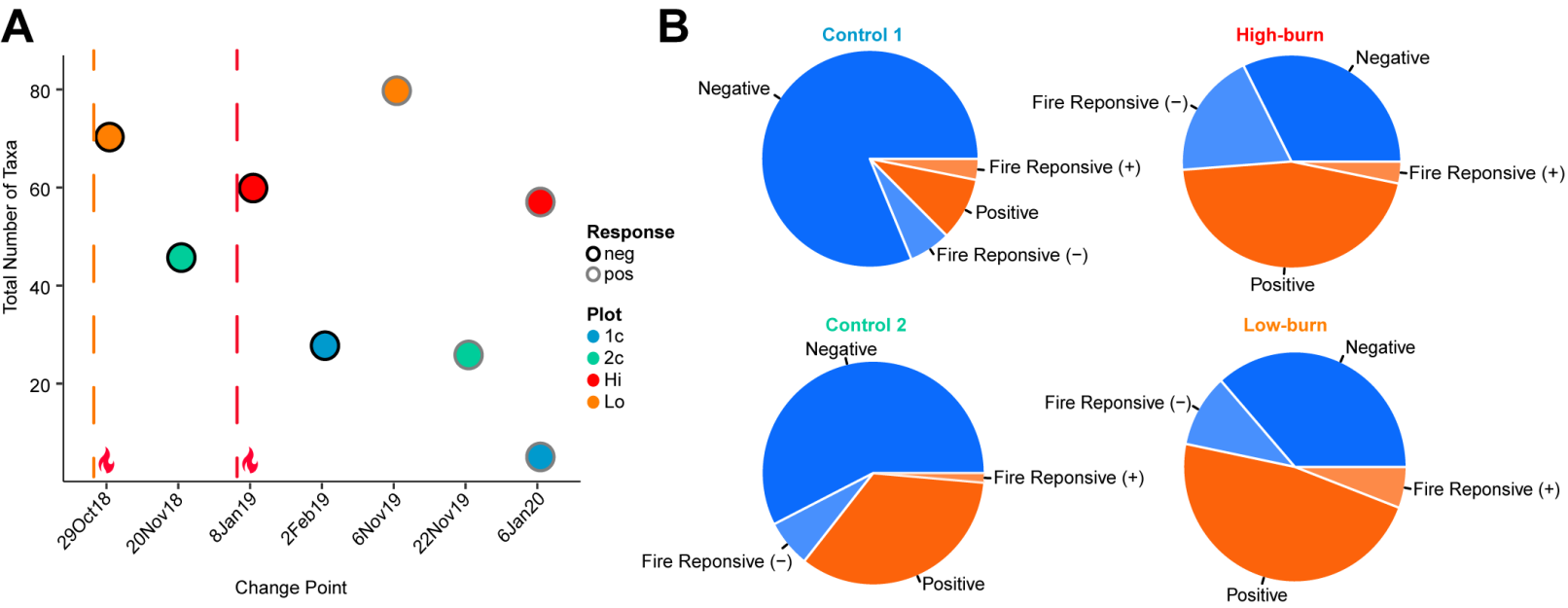

Figure 4

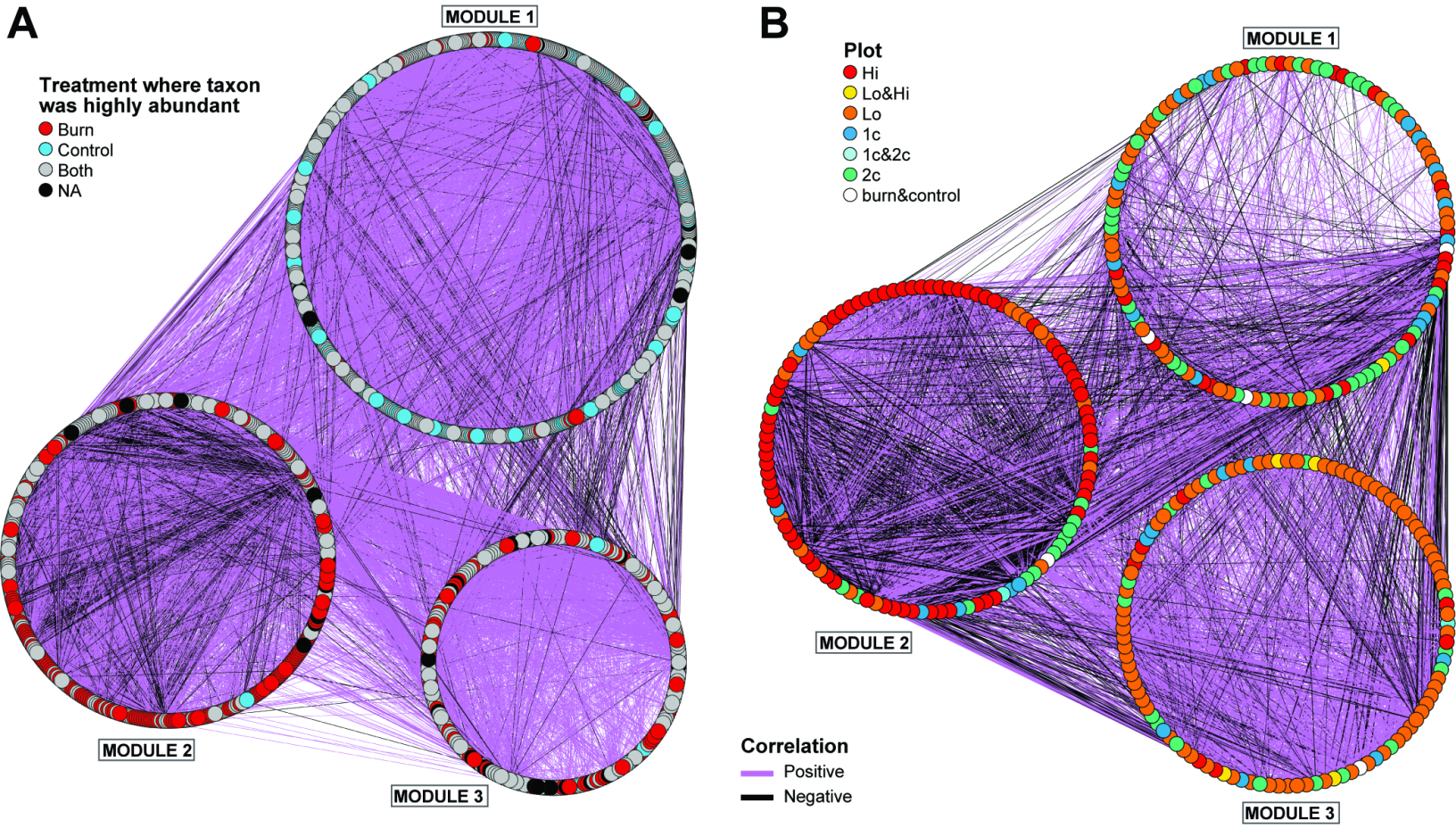

Figure 5

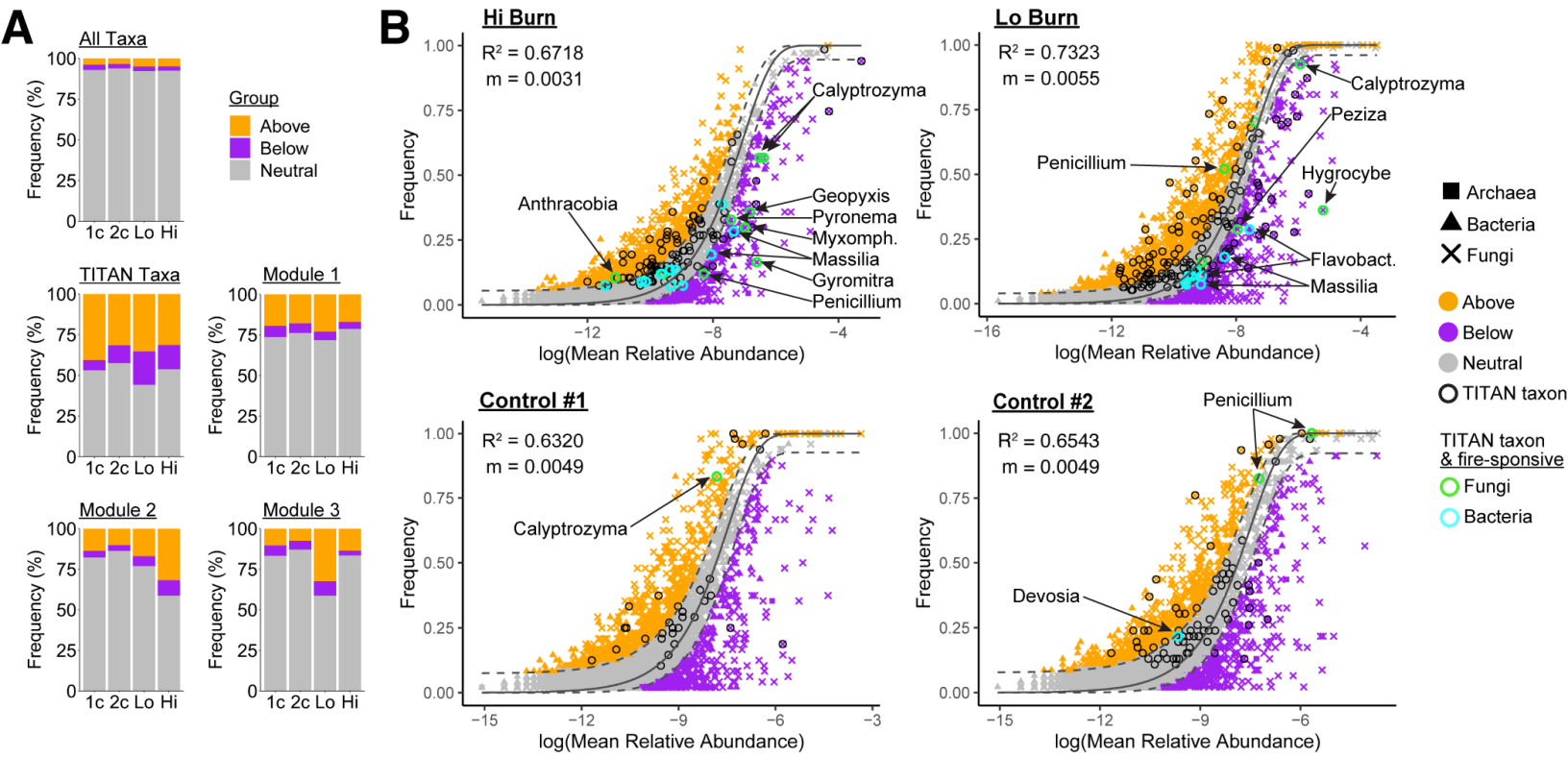

Figure 6